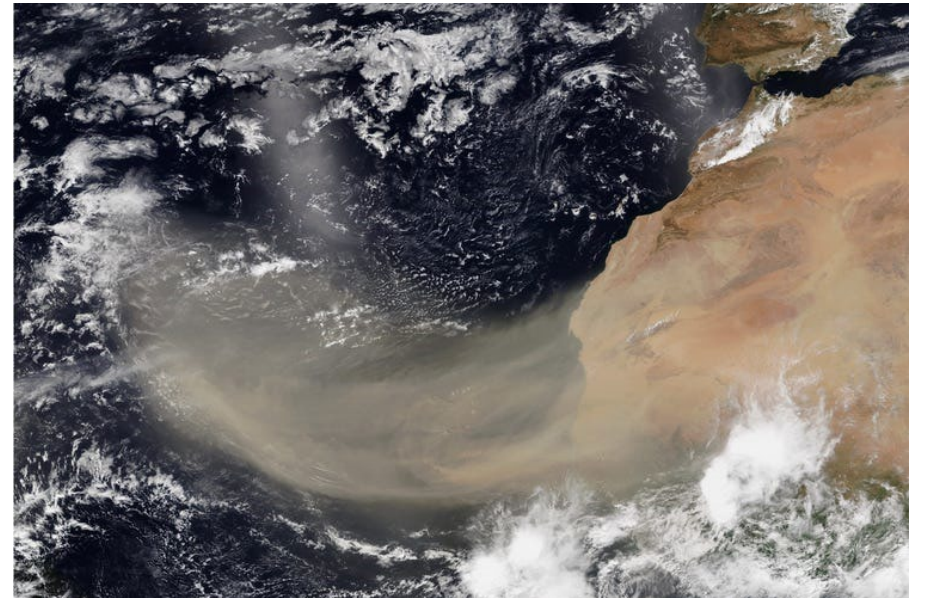


A historical dust emission dataset for better evaluating aerosol radiative forcings: A climate perspective

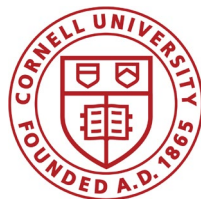
AMWG winter meeting
13 Feb 2024

Danny M. Leung^{1,2}, Jasper Kok², Longlei Li³,
Natalie Mahowald³, David Lawrence⁴, Simone Tilmes⁵,
and Erik Kluzek⁴

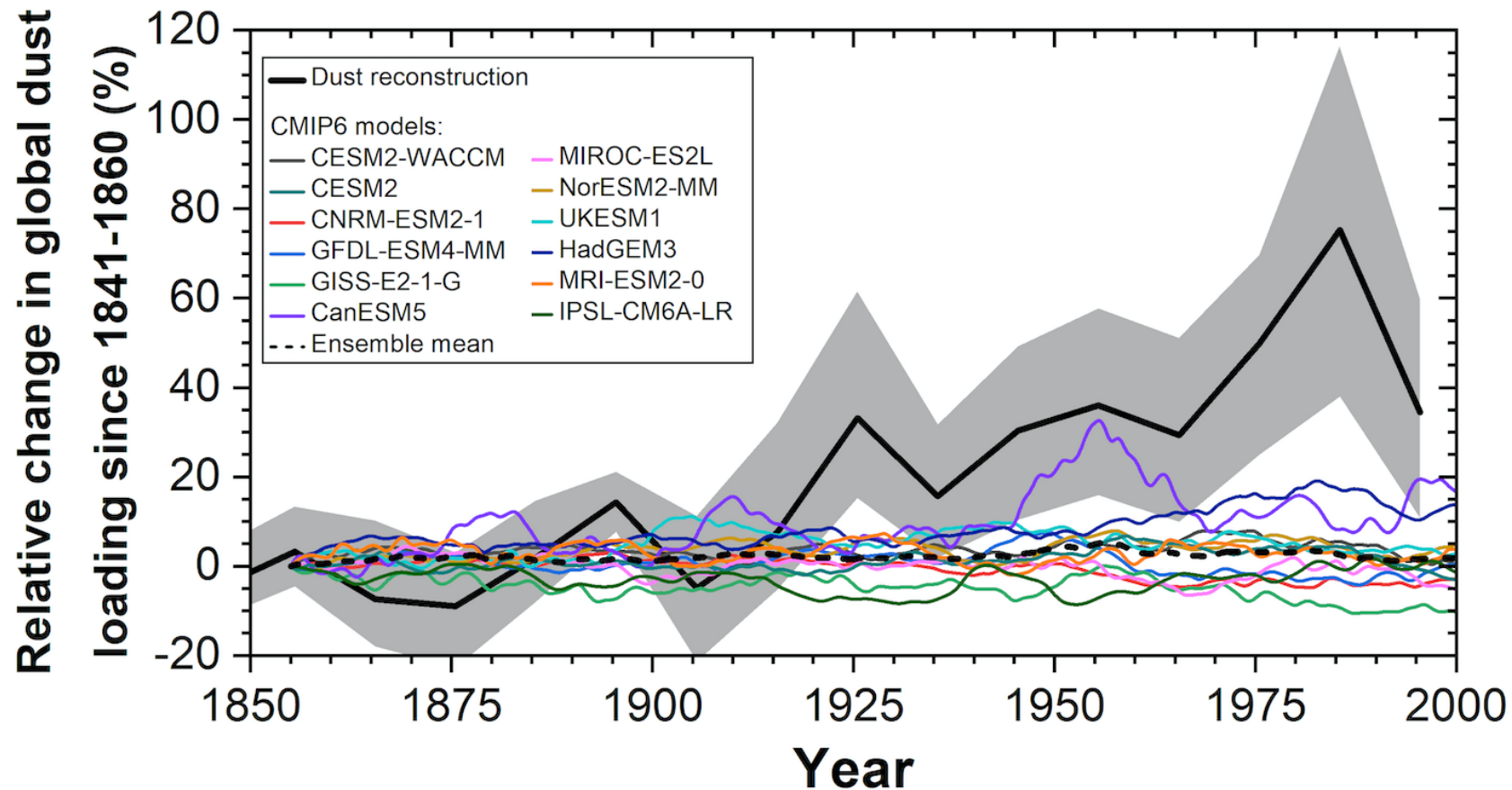
¹ASP | ²UCLA | ³Cornell | ⁴CGD | ⁵ACOM



NASA worldview MODIS aerosol image for the
Godzilla dust event, 18 June 2020



Climate models fail to capture the observed historical dust trend.



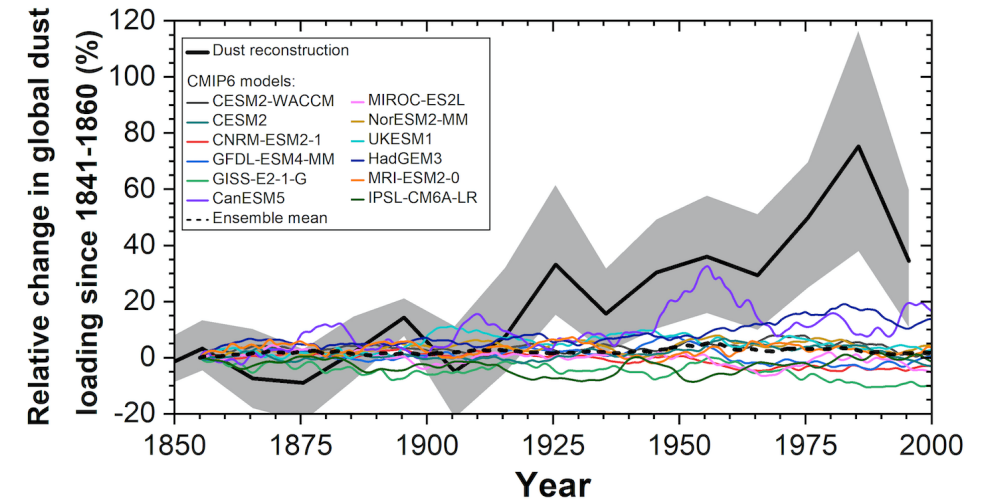
Kok et al. (2023)

- Current ESM aerosol mechanistic emission schemes (e.g., dust, fire) are calibrated toward **present-day** observations; they **cannot be extrapolated to other climates**.
- However, this is what modelers are doing now (e.g., in CMIP runs).
- CMIP6 ESMs **could not replicate the historical ~50 % increase** in dust for 1850–2000 as indicated by multiple sedimentary records of dust deposition fluxes. Ramifications?

To better evaluate aerosol radiative forcings, we need ESM aerosols to follow historical observational constraints.

Ramifications of little historical dust change in ESMs:

- ESMs underestimate the historical aerosol radiative forcings (RFs).
- **Missing dust RFs (cooling)** to counteract historical warming in ESMs.
- ESMs need these aerosol RFs to better evaluate the **climate sensitivity**.



The historical dust increase was likely due to land use land cover change (LULCC) and climate change, but currently it remains a challenge to model the dust–LULC–climate interactions.

Two proposed approaches to force ESM dust to follow the observed historical variability:

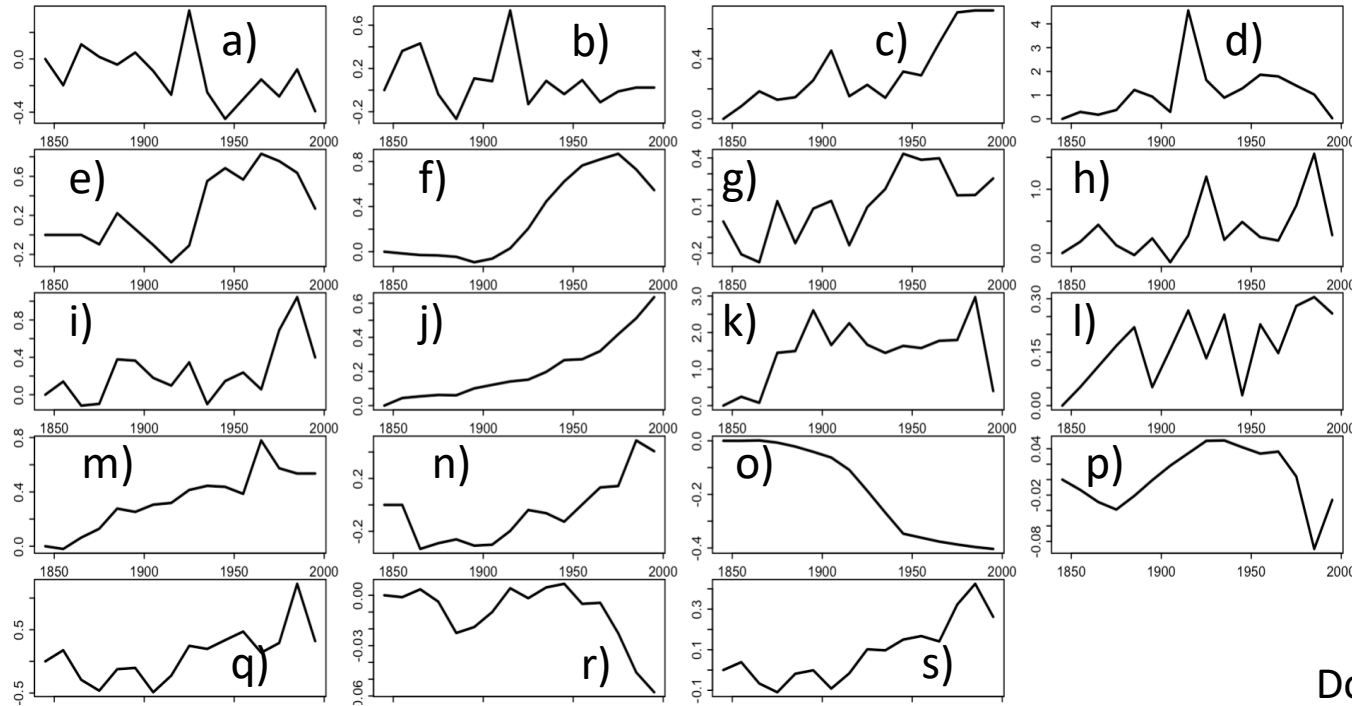
- 1) ESMs use the observed historical constraint to tune dust; set 2000s dust to a global mean of 0.03 (Ridley et al., 2016), and obtain **dust emission tuning factor** back to the 1850s (**constraining globally**);
- 2) We use the sedimentary records to optimize a **global dust emission dataset** for 1850–2000 (**constraining regionally**).

In this talk we focus on the derivation of (2) and its preliminary evaluation in the CESM2.

Method: Using 19 dust deposition records to constrain 9 regional dust emissions decadal.

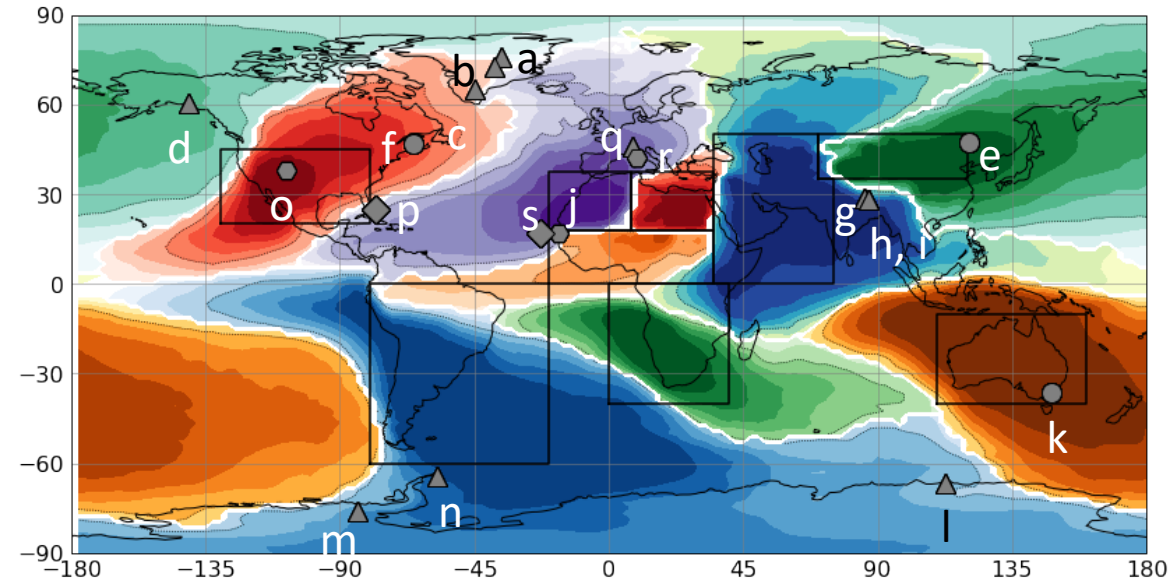
Normalized decadal dust deposition time series for 1840–2000

β_j for $j = [1, \dots, 19]$



Sources: McConnell et al. (2007), Mulitza et al. (2010), Mahowald et al. (2010), Hooper and Marx (2018), Clifford et al. (2019)...

Deposition record sites and dominant source regions



Dots: site locations

Rectangles: defined regions for estimating regional emissions

Colors: fraction of the dust deposition supplied by different dominant source regions (from global model simulations)

Goal: optimize regional emissions λ_i for all 9 defined source regions $i = [1, \dots, 9]$ using observed dust deposition $j = [1, \dots, 19]$.

Schematic for using the observed dust depositions to derive the DustCOMM v1 emissions

1. An ensemble of bias-/observation-corrected model (CESM1, GEOS-Chem, IMPACT, ...) simulations of **Jacobian matrix** f_{ij} relating **dust deposition** β_j at the j^{th} site/grid to the **regional emission** λ_i at the i^{th} region:

$$f_{ij} = \frac{\partial \beta_j}{\partial \lambda_i}$$

for $j = [1, \dots, 19], i = [1, \dots, 9]$



2. Sedimentary records of deposition flux time series $\beta_j(d)$ for $j = [1, \dots, 19]$ where d is any decade within 1840–2000.



3. Optimize/invert $\lambda_i(d)$ for $i = [1, \dots, 9]$ in any decade d by minimizing the cost function:

$$\chi(d)^2 = \sum_{j=1}^{N_{\text{dep}}} \left[\sum_{i=1}^{N_{\text{SR}}} \lambda_i(d) f_{ij} - \beta_j(d) \right]^2$$



6. multiply the normalized $F_i(\theta, \phi)$ by $\lambda_i(d)$ (as **weights/relative importances**) and summing up:

$$F_{\text{DustCOMM}}(\theta, \phi, d) = \sum_{i=1}^{N_{\text{reg}}=9} \lambda_i(d) F_i(\theta, \phi)$$

$F_{\text{DustCOMM}}(\theta, \phi, d)$: **DustCOMM** emission dataset.



5. We borrow regional dust emissions $F_i(\theta, \phi)$ from the ESM ensemble (for the 1990s); Normalize the regional $F_i(\theta, \phi)$ maps to a regional total of **unity**

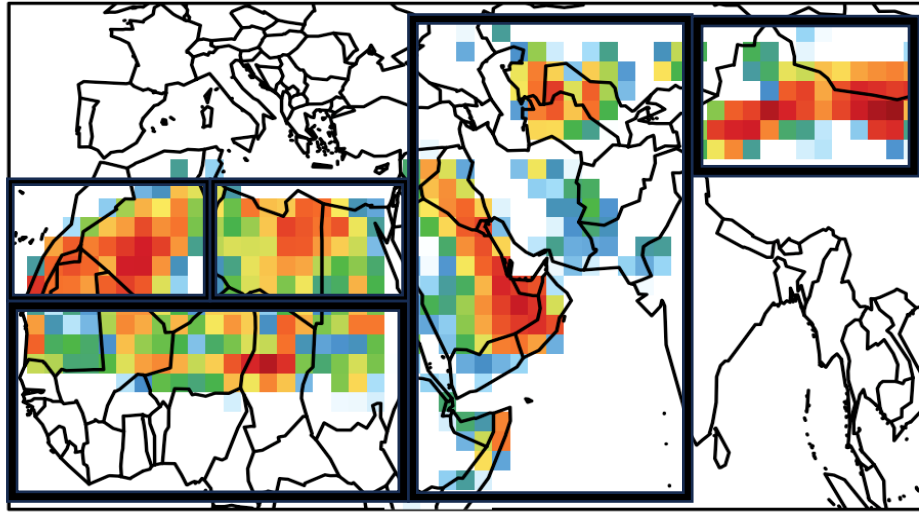


4. Obtain regional total emissions $\lambda_i(d)$ for all i regions as decadal time series.

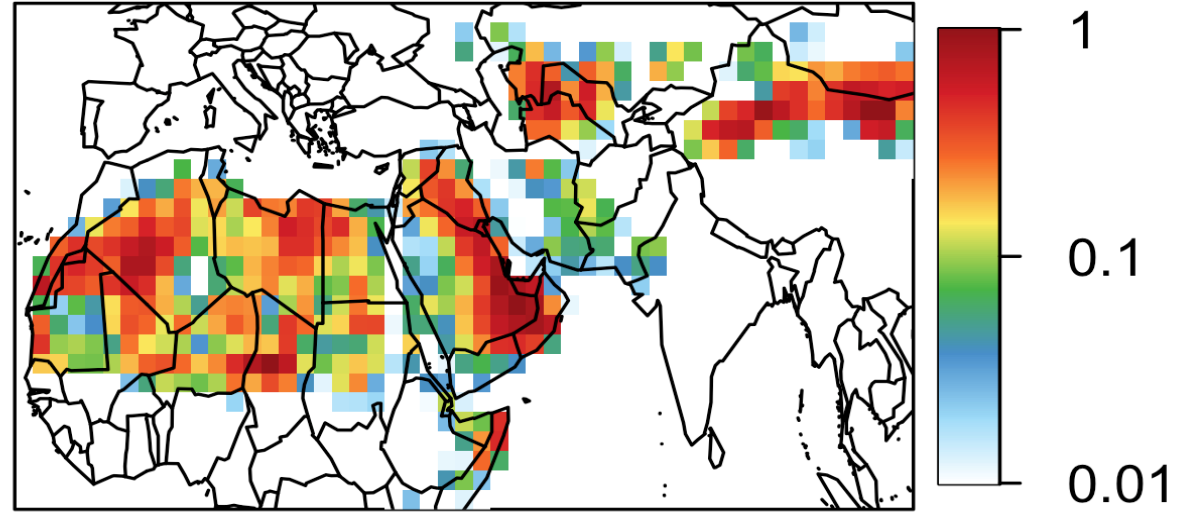
Regional optimization; no subregional optimization.
Higher-resolution inversion in the future versions..

The DustCOMM (v1) dust emissions

1851–1870 emissions over the Dust Belt



1981–2000 emissions over the Dust Belt



- horizontal resolution: 1.9°x2.5° (resolution of the ESM ensemble)
- Coverage: 1841–2000; global total emission increased ~50 % across 1850–2000.
- Each defined region has their own decadal varying emissions, optimized by the interdecadal variability of the sedimentary records.
- The subregional spatial emission variability remains the same across time (since it is the same ESM ensemble mean).

Model for our study: CESM2.2

Compset: FHIST (transient land + atmosphere coupled; other ES components inactive)

Land: Community Terrestrial System Model (CTSM5) Satellite Phenology (SP) mode

Atmosphere: Community Atmosphere Model (CAM6) + Modal aerosol model (MAM4)

Dynamics: FV dycore

Resolution: 0.9°x1.25°x32 (-f09_f09_mg17, -nlev 32)

Timestep: 30 minutes

Simulation period: 1851–2000

Evaluating the CESM2–DustCOMM run: CTSM5 emissions and CAM6 dust AOD

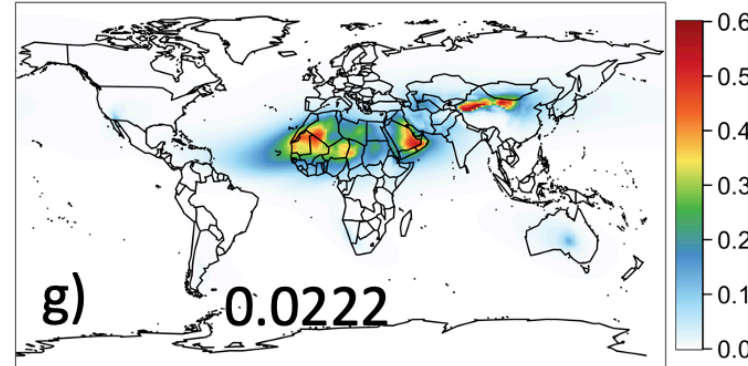
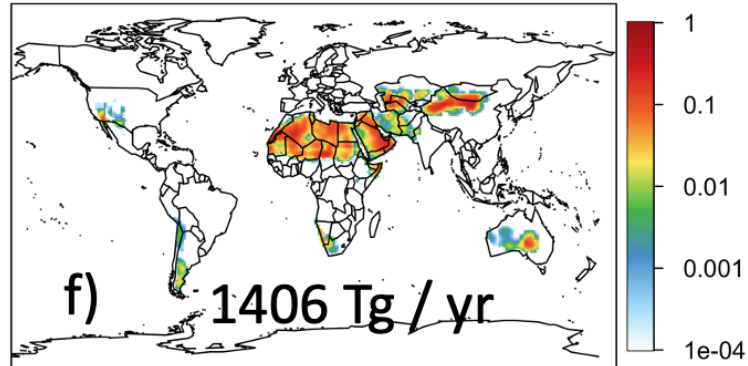
Spatial variability

Interannual/Interdecadal variability

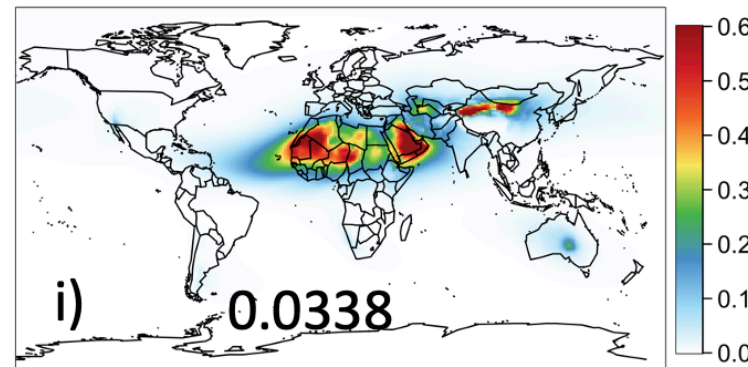
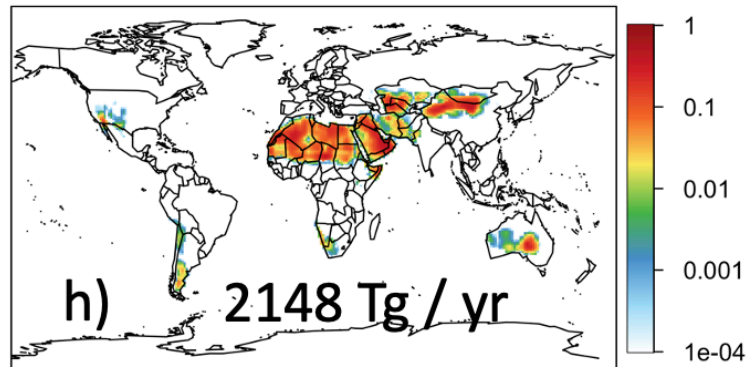
CTSM5 emissions

$\text{kg m}^{-2} \text{yr}^{-1}$ CAM6 DAOD

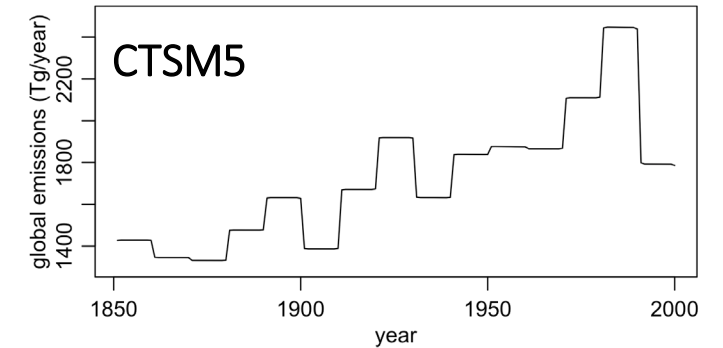
1851–1870



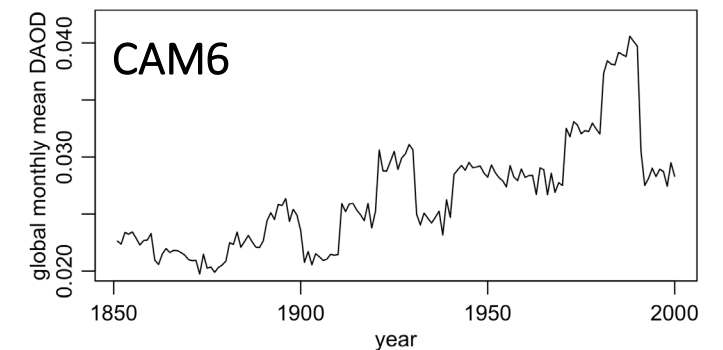
1981–2000



Annual mean global total emission



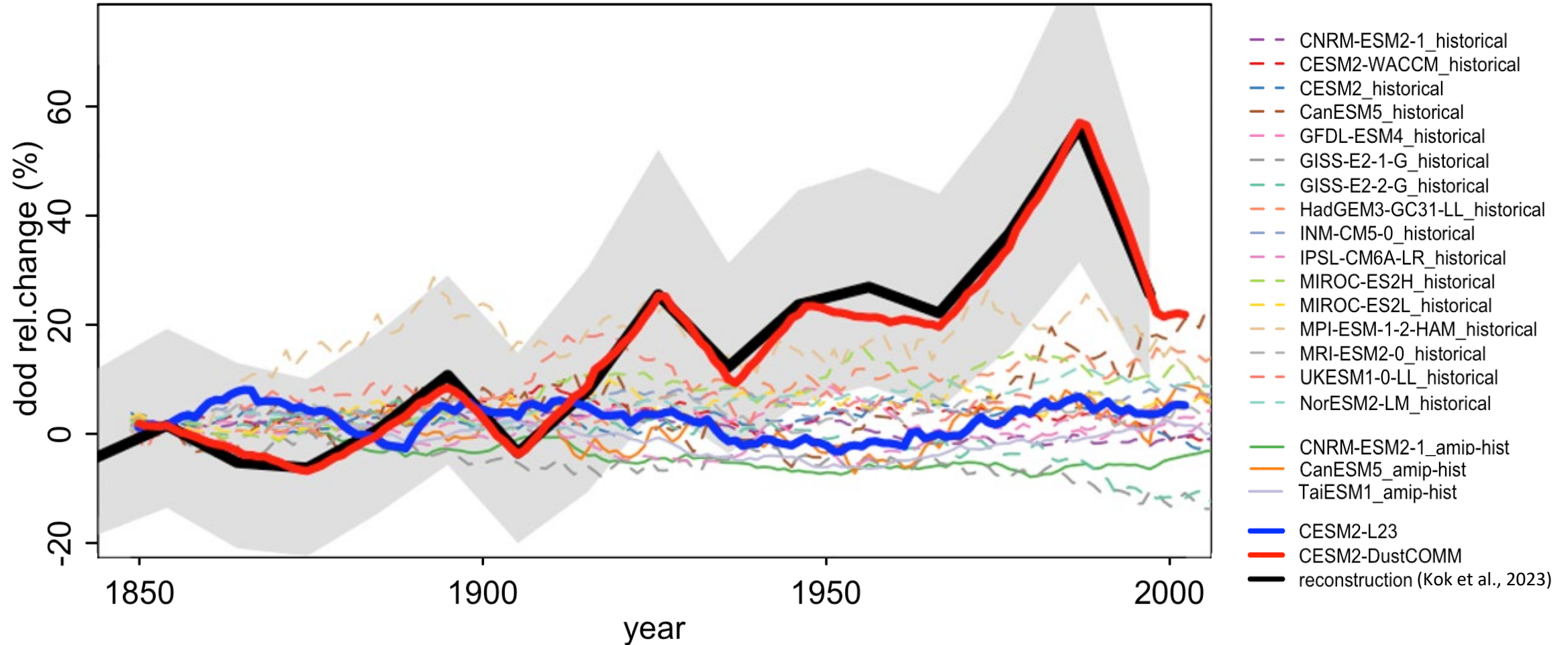
Annual mean global mean DAOD



The CTSM emissions and CAM6 dust AOD followed the DustCOMM emission to increase with time by $\sim 50\%$.

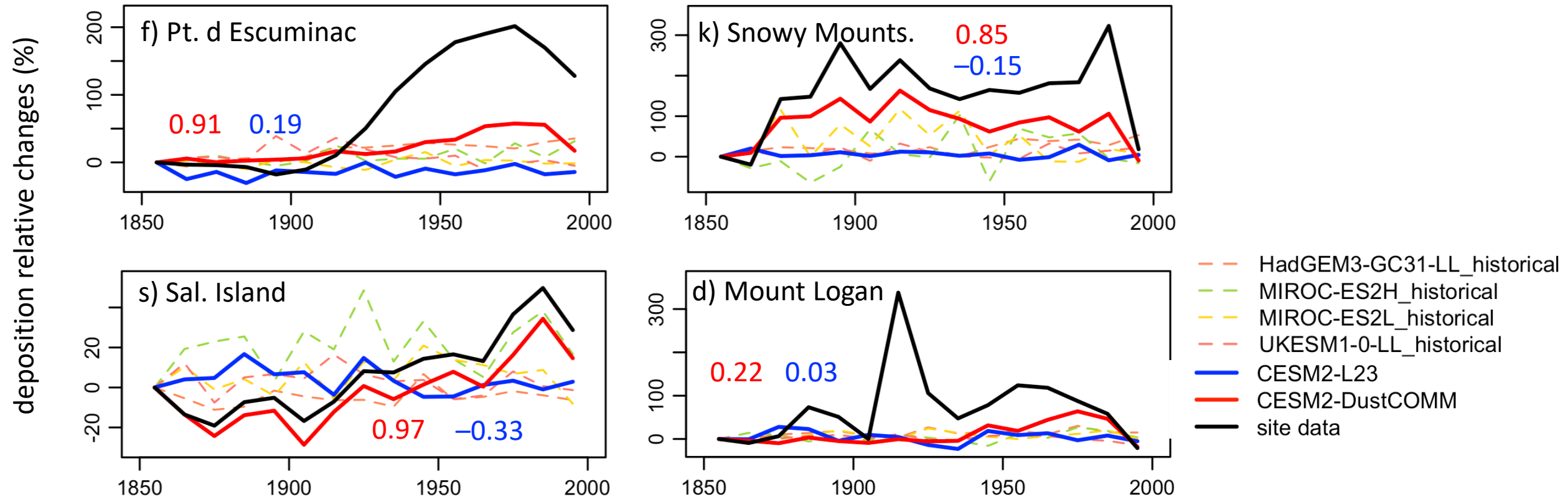
1851–2000 dust aerosol optical depth from our CESM2 runs and CMIP6 runs.

10-year running mean global mean DAOD percentage change since the preindustrial period



Only the CESM2–DustCOMM run’s dust AOD can match the interdecadal variability of the K23 reconstructed DAOD derived from the sedimentary records of dust.

CESM using the DustCOMM emissions overall capture better the interdecadal variability of dust deposition fluxes than ESM runs using mechanistic emission schemes.



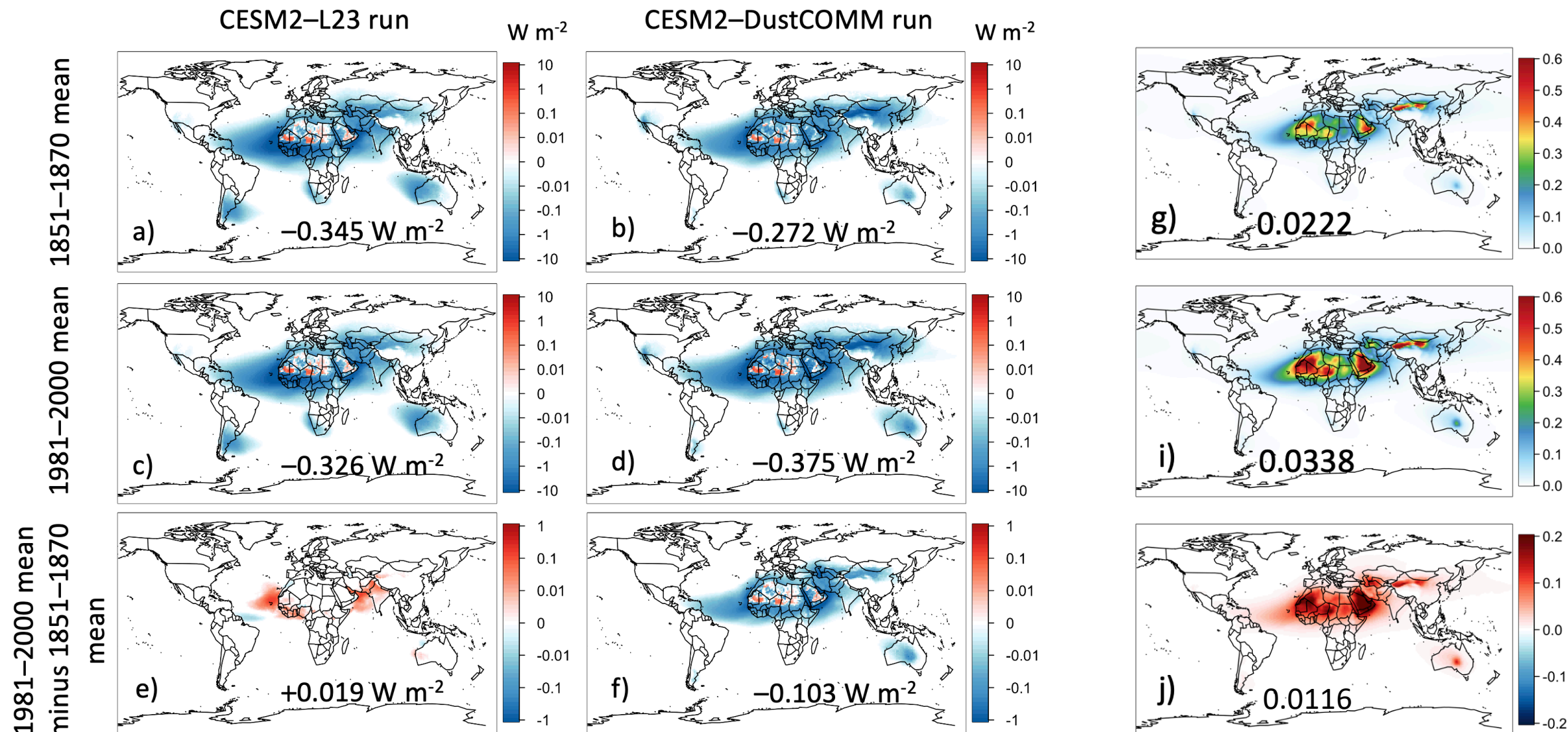
CESM2–DustCOMM does not necessarily reproduces the deposition time series well because of

- (i) representation error (grid vs. site),
- (ii) weakened emission variability during the optimization (variability across different sites partially offset each other).

1981–2000 minus 1851–1870 dust direct radiative effect (RE) using Leung 2023 and DustCOMM emissions.

Direct radiative effect/forcing

CESM2–DustCOMM dust AOD



Note that CESM2–MAM4 only include dust PM up to 10 μm .

Summary

1. CMIP6 ESMs generate little or no trends in historical dust, as the mechanistic dust schemes are calibrated towards present-day observations and cannot extrapolate well.
2. CESM–DustCOMM historical run gives 1990s minus 1850s historical direct dust RF is -0.1 W m^{-2} ; the direct RF of all aerosols is $-0.45 \pm 0.5 \text{ W m}^{-2}$ (90 % CI; Bellouin et al., 2020).
3. We are working on a PR to make the DustCOMM dataset available in CTSM.
4. If using mechanistic emission schemes, we suggest following the global dust constraint: Using the [time-varying dust tuning factor to reproduce the observed 1850–2000 dust increasing trend](#), for better ESM evaluations of [aerosol RFs and climate sensitivities](#).
5. Aerosol modelers are currently using the DustCOMM emissions to evaluate the 1850–2000 dust RFs (AeroCom phase III, ongoing). The DustCOMM emissions might also go into CMIP7 (AerChemMIP2 and/or AerHistMIP; Jasper Kok, Natalie Mahowald)

